On Fingerprint Template Synthesis

Wei-Yun Yau, Kar-Ann Toh, Xudong Jiang, Tai-Pang Chen and Juwei Lu

Centre for Signal Processing
School of Electrical & Electronic Engineering
Nanyang Technological University

Abstract

In this paper, we address the false rejection problem due to small solid state sensor area available for fingerprint image capture. We propose a minutiae data synthesis approach to circumvent this problem. Main advantages of this approach over existing image mosaicing approach include low memory storage requirement and low computational complexity. Moreover, possible overhead on the search engine (for fingerprint matching) due to data redundancy could be reduced. Extensive experiments were conducted to determine the best transformation suitable for minutiae alignment. We demonstrate the idea of synthesis with an example using physical fingerprint images. The proposed synthesis system is also found to improve (lower) the number of false rejects due to the use of different fingerprint regions for matching.

keywords:-
Biometrics, image database, fingerprint identification, fingerprint verification, minutiae points, template matching.

1 Introduction

In general, an automatic fingerprint identification or verification (see e.g. [1, 2, 3, 4]) system consists of three main processing stages namely, *image acquisition*, *feature extraction* and *matching*. In image acquisition, query and template database images are acquired through various input devices. Development over the years has seen through means that mechanically scan the ink based fingerprints into the computer system, and means which directly capture the fingerprints using more sophisticated solid state sensors. With fingerprint images which could be distorted or contaminated with noise, the automated system seeks to *extract* characteristic *features* which are discriminating and yet invariant with respect to image orientation. The final stage of fingerprint identification or verification is to search and verify matching image pairs.

The use of inkless sensors has advanced the data acquisition aspects in an automatic fingerprint identification/verification system. This includes optical and solid state devices. By means of CCD array and laser technologies, the optical sensors offer a cost effective solution for fingerprint image capture. Conforming to the regulation by National Institute of Standard and Technology (NIST, USA), conventional optical sensors have a sensing area of 1-inch by 1-inch. The solid state sensors, which adopt capacitance, electric field, pressure or temperature sensing technologies, offer a more compact means for fingerprint image capture with additional features to detect presence of fingers such as locally adjustable automatic gain control [5]. However, due to manufacturing limitation and cost factors, most solid state sensors do not come with large sensing area (e.g. Veridicom's *i*Touch has a sensing area of 1.5cm by 1.5cm and Infineon's FingerTip has a sensing area of 11.1mm by 14.3mm). Moreover, the imaging area for the finger is further restricted to the area in contact with the sensor. This, as compared to conventional ink based rolled fingerprint impression, possesses a much smaller information area. A consequence of this can be seen in using different partial areas of the same finger for matching, which causes false rejection. For this reason, during enrollment of a person in a database, a rolled fingerprint would be preferred over a plain touch impression.

Apart from requiring the individual user to ensure good placement of fingerprint area during image acquisition process, few automatic fingerprint identification/verification system has addressed the problem of false rejection cause by using different image regions for matching. While acquiring a few separate fingerprint images during registration could simply handle the false rejection problem, much of the acquired information could be redundant (due to much common regions) and hence takes up unnecessarily large storage space. Moreover, overheads of the multi-modal search would increase due to the much larger number of records available for matching. In [6], an image mosaicing technique is developed for constructing a rolled fingerprint from an image sequence of partial fingerprints. The proposed fingerprint mosaicing algorithm consists of four stages namely, (i) segmentation of foreground and background areas in each frame; (ii) weighting of each image's contribution using a foreground mask; (iii) stacking of the weighted gray scale frames to compute the mosaic gray scale image; (iv) stacking of the foreground masks to compute a confidence index at every pixel. Although mosaicing technique possesses the capability of acquiring a larger area of fingerprint image, it is at the expense of large storage requirement for a much larger synthesized image. Moreover, as seen from the pixel level computation which is applied directly to the acquired image, the computational cost is high.

In this paper, we propose a minutiae based synthesis method for an automatic fingerprint identification/verification system. The proposed methodology not only synthesize necessary information for fingerprint identification, but also possesses several desired features:

1. no restriction on the hardware sensor area;

2. small storage requirement since the synthesized data contains only the necessary minutiae information needed for matching. This is especially useful for search within a large database in fingerprint identification;

3. low computational complexity.

The paper is organized as follows: in section 2 we provide a brief overview on fingerprint identification and verification problems related to the subject matter. This is followed by section 3 where our representation system for minutiae data and our methodology for minutiae synthesis are presented. Section 4 provides an outline on minutiae detection, minutiae alignment and several transformations available for minutiae alignment. In section 5, we perform experimental study to decide upon the best transformation for our application. Then, on top of a minutiae synthesis example, we provide an evaluation of

the synthesis system in aspects of false rejection. Some concluding remarks are drawn in section 6.

2 Fingerprint Identification/Verification

While *fingerprint identification* refers to the process of matching a query fingerprint against a template fingerprint database to establish the identity of an individual, *fingerprint verification* refers to determination of whether two fingerprints are from the same finger or not. Since verification is a comparison of a *query* fingerprint against an enrolled *template* fingerprint, it is also termed as *one-to-one matching*. Identification, on the other hand, is termed as *one-to-many matching*.

In view of effective search within a huge database in an identification problem, fingerprint matching is usually carried out at two levels namely, the coarse level and the fine level. The coarse level matching is also referred to as classification (see e.g. [7, 8, 9, 10]) where fingerprints are grouped into few classes so that a fine level search can be performed within the matched class.

As it is difficult to use the raw digital fingerprint image directly for matching in an automatic fingerprint identification/verification system, a suitable computer representation is essential. Several desirable properties for such representation can be identified as:

1. retention of the discriminating power of each fingerprint (information content),

2. stable with respect to noise and distortion,

3. small in data storage size, and

4. ease in manipulation (e.g. adding new data points).

Here, we note that large information content may pose a constrain to small data storage size requirement.

According to [11], eighteen different types of fingerprint features can be identified. These features include ridge endings, ridge bifurcations, short ridges and ridge crossovers which are collectively termed as *minutiae*. It has been widely accepted that local ridge structures (a collection of minutiae details) from two fingerprints match each other if the fingerprints are from the same source [11, 12]. Hence, the problem of fingerprint verification can be reduced to a point pattern matching problem when these local structures are considered.

3 Minutiae Data Synthesis

Our representation for the fingerprint consists of a global structure and a local structure [13]. The global structure consists of positional and directional information of ridge endings and ridge bifurcations. The local structure consists of relative information of each detected minutia with other neighboring minutiae. Since the local structure contains relative information which is insensitive to rotation and translation, the main issue concerning minutiae data synthesis is to establish the relationship between the global structures of two fingerprints acquired with common regions.

Let

$$M = \{(x_i, y_i, \varphi_i, t_i)\}, \ i = 1, 2, ...n \qquad (1)$$

be the set of minutiae containing the positional information (x, y), directional information (φ) and minutiae type information ($t_i = 0$ indicates a ridge ending and $t_i = 1$ indicates a bifurcation) for n minutiae elements in the global structure.

Suppose we have a total of m number of minutiae data sets from m partial fingerprints of the same finger, then

we can write for the kth minutiae data set as:

$$M_k = \{(x_i, y_i, \varphi_i, t_i)\}_k, \ i = 1, 2, ...n_k, \ k = 1, 2, ..., m. \qquad (2)$$

Among these minutiae data sets, there would be common regions whereby information is redundant. If it is to search through each individual minutiae data sets for matching, it would not be cost effective since these redundant information are being searched through more than once. Moreover, the geometrical relationships among these minutiae data sets are no longer preserved since these data sets are treated as separate entity. In order to save data storage space with respect to redundancy as well as to provide a good overall picture about the minutiae sets, a synthesis with consideration to relationship between data sets is needed.

For fingerprint images with common regions, we can express the resultant synthesized information as:

$$M_{\cup_1^m} = \bigcup_{k=1}^{m} \{f_k(x_i, y_i, \varphi_i, t_i)\}_k, \ i = 1, 2, ...n_k \qquad (3)$$

where $f_k, \ k = 1, 2, ..., m$ denote the necessary topological transformations for aligning the different sets of minutiae data. Suppose o_1 is the number of overlapping points between M_1 and M_2. Then the number of minutiae points in $M_{\cup_1^2}$ can be expressed as $n(M_{\cup_1^2}) = n_1 + n_2 - o_1$. Now let o_2 be the number of overlapping points between $M_{\cup_1^2}$ and M_3. And the number of minutiae points in $M_{\cup_1^3}$ is $n(M_{\cup_1^3}) = n_1 + n_2 + n_3 - o_1 - o_2$. In short, the total number of minutiae points in the synthesized minutiae data set $M_{\cup_1^m}$ can be written as:

$$n(M_{\cup_1^m}) = \sum_{k=1}^{m} n_k - \sum_{k=1}^{m-1} o_k, \qquad (4)$$

where o_k is the number of overlapping minutiae points between $M_{\cup_1^k}$ and M_{k+1}. Hence, if each o_k is of considerable size, the total number of minutiae in the synthesized data set ($n(M_{\cup_1^m})$) can be significantly smaller than $\sum_{k=1}^{m} n_k$.

Upon acquiring two images for synthesis, the task immediately after minutiae detection is to find correspondence between these two images so that the global minutiae information between the two images can be aligned. A match between these two images is performed utilizing both local and global minutiae information. Two minutiae data sets are considered matched if a weighted score between the local and the global information exceeds a certain threshold value. The match shall reject the input image if the intersecting region is too small for good correspondence. We shall discuss our alignment method in a separate section.

Let M_j and M_k, $j \neq k$, $j, k \in \{1, 2, ..., m\}$, be two fingerprint minutiae data sets to be synthesized. Suppose there are p corresponding points (minutiae coordinates) between the two images. Denote this set of p corresponding points by C. Then, a topological transformation f can be determined relating M_j and M_k from

$$x_j = f(x_k) \qquad (5)$$

where $x_j = \{(x_i, y_i)\}_j$ and $x_k = \{(x_i, y_i)\}_k$ for all $i \in C$. Since the transformation will be used for aligning those non-corresponding minutiae points, a careful study on its sensitivity with respect to noise and deformation is necessary. We shall discuss various transformation models for image points alignment in the following section.

4 Minutiae Detection and Alignment

For minutiae detection, we adopt an adaptive ridge tracing algorithm which is evolved from [14]. Our approach

adaptively traces the gray-level ridges of the fingerprint image and applies adaptive oriented filters to the image only at those regions that require to be smoothed. A long tracing line will be obtained when there is little variation in contrast and when the bending level of the ridge is low. Main advantage of our approach is that tracing is by *adaptive* piece wise linear approximation of the ridges which speeds up the process of ridge detection as compared to other methods which adopt either pixel wise or fixed step tracing [15]. The tracing is only performed within the region of interest. The region of interest is segmented based on the local certainty level $c(x, y)$ at pixel (x, y) on image I.

Several stopping criteria for ridge tracing which determines detection of minutiae are adopted as:

1. Tracing exits from region of interest. In this case, minutiae extraction will not be performed.

2. Tracing ridge line intersects another already traced skeleton ridge line. Under this condition, a bifurcation minutiae is detected.

3. Tracing ridge line ends when the tracing line is shorter than a threshold value and when the next traced point lies on another ridge.

In addition to minutiae detection, post processing is performed to remove spurious minutiae.

Having the minutiae extracted for two images, it is necessary to align the two sets of data so that they form a larger picture of the fingerprint. Several problems which are inherent to this alignment process are enumerated as follows:

1. Translation and rotation variance between the two fingerprint images.

2. Some minutiae may be dropped and some spurious minutiae may be detected.

3. Deformation of the fingerprint images which induces location errors.

Together with an indication of ridge ending and ridge bifurcation, the notation in (1) provides a global description of the minutia. Since this feature vector is not rotation and translation invariant, we construct a local feature vector for our alignment purpose. In what follows, only a brief outline on the local structure for alignment matching will be provided. The interested reader is referred to [13] for greater details.

Let m_j, $j = 1, 2, ..., l$ be the jth nearest neighbour with respect to m_0. The distance between m_0 and m_j can then be expressed as

$$d_{\mathsf{j}\,0} = \sqrt{(x_\mathsf{j} - x_0)^2 + (y_\mathsf{j} - y_0)^2}. \qquad (6)$$

Denote by φ_0 the direction of m_0, the relative radial angle for m_j with respect to m_0 is given by

$$\theta_{\mathsf{j}\,0} = \tan^{-1}\left(\frac{y_\mathsf{j} - y_0}{x_\mathsf{j} - x_0}\right) - \varphi_0, \quad -\pi \leq \theta_{\mathsf{j}\,0} \leq \pi. \qquad (7)$$

Let $c_{\mathsf{j}\,0}$, $j = 1, 2, ..., l$ be the ridge count between m_0 and m_j, then together with corresponding minutiae type $t_{\mathsf{j}\,0}$ we pack the local feature vector as

$$F_{\mathsf{l}\mathsf{j}} = [d_{\mathsf{j}\,0}, \theta_{\mathsf{j}\,0}, c_{\mathsf{j}\,0}, t_{\mathsf{j}\,0}]^\mathsf{T}, \quad j = 1, 2, ..., l. \qquad (8)$$

It is obvious that this local structure is rotation and translation invariant since it contains only relative information. Hence, it can be used directly for preliminary local alignment matching.

A match weighting the similarity between the local feature vectors from the two images is performed so that a common reference can be established. Once the preliminary correspondence between these local features is established, the transformation required for global alignment can be found. To validate good correspondences

for this transformation, a further match combining both local and global information is adopted.

Generally, transformation means can be classified in linear form and nonlinear form. Consider two sets of image points: $\mathsf{x} = (x, y)$ and $\mathsf{X} = (X, Y)$. The problem here is to find the best transformation f that relates these two sets of image points, i.e. $\mathsf{x} = f(\mathsf{X})$. For linear transformations, we have $\mathsf{x} = \mathsf{T}\,\mathsf{X}$ where T denotes the transformation matrix.

Affine geometry compares distances only on the same line or on parallel lines. As compared to the Euclidean geometry, affine geometry relaxes the requirement on perpendicularity. Hence transformation under affine geometry is more general as compared to that under Euclidean geometry.

Projective geometry is the result of relaxing the restrictions preserving parallel lines but require that straight lines remain straight lines for any changes we might impose on the figure.

Topology encompasses the projective, affine and Euclidean geometries. An even smaller set of properties is invariant under topological transformation (e.g. preserving only closed curves, order and connectivity). Here, only the quadratic type of topological transformation is investigated.

5   Experiments

5.1   Transformation study

In this section, we perform experimental study, using physical fingerprint data, to determine a suitable transformation for minutiae synthesis. We collect 5 images corresponding to 5 different areas (centre, top-left, top-right, bottom-left and bottom-right) for each finger for the experiment. A total of 200 images were captured using the *Veridicom Sensor* for 40 fingers.

Matching was first performed to obtain the corresponding coordinates between two images which are to be synthesized. We used the centre area as the base image to match with one of the other areas (top-left, top-right, bottom-left and bottom-right) of the same finger. The matched image pairs with 10 or more corresponding minutiae coordinates were then used for the following transformation study. As a result, only 50 matched pairs were found to have 10 or more matched points.

To assess the accuracy of each transformation discussed in previous section, 3/4 of the matched points were used for identifying the transformation parameters (fitting) and the rest of 1/4 were used for extrapolation test (testing). The distribution of the sum of squared errors (SSE) for these matched pairs are plotted in Fig. 1 and Fig. 2 for fit data and test data respectively. The continuous line ('___') corresponds to SSE distribution for *affine transformation*. The dashed line ('- -') and the dotted line ('...') correspond to *projective transformation* and *topological transformation* respectively. The mean value and the standard deviation (STD) for these errors are also tabulated in Table 1 to reflect an overall view of these results.

As seen from Fig. 1, the topological (quadratic) transformation provides the best fit since the dotted curve falls below the other two curves for all samples. This is also reflected in Table 1 since the mean SSE and the standard deviation (STD) are the smallest among the three transformations. As for test data not included in the fitting process, results from Fig. 2 and Table 1 show that affine transformation gives the best result, in the sense of lowest mean SSE and lowest STD. It is important to note that both the mean SSE and STD for the other two transformations (projective and topological) are considerably huge as compared to those by affine transformation. Main reason being that coordinate warping according to
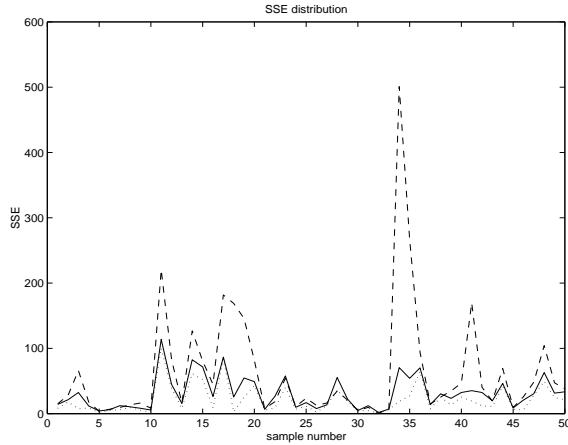
Figure 1: Sum of squared error distribution for fit data
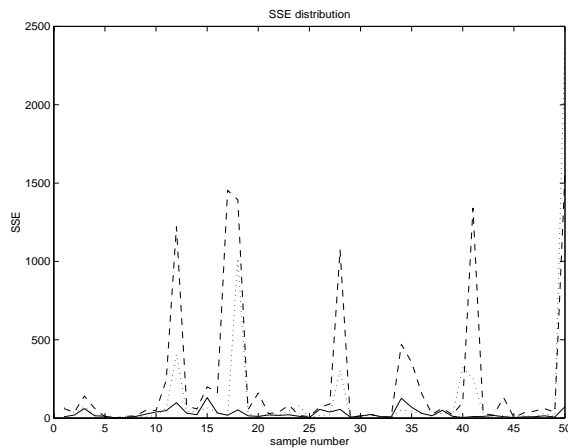
Figure 2: Sum of squared error distribution for test data

the fit data (interpolation) may not necessary fit well the test data (extrapolation). Base on this study, the affine transformation is adopted for alignment in our minutiae synthesis system.

5.2 A minutiae synthesis example

In this part, we show an example of synthesizing three fingerprint images. As shown in Fig. 3 through Fig. 5, three fingerprint images are captured from three different portions of the same finger. Minutiae points (shown in circles in Figures 3-5) are detected from these fingerprint images using the ridge tracing algorithm. A visual examination on these figures shall reveal that the minutiae information extracted in each image contains similar points (found in common regions) and dissimilar points (found outside common regions). It is also observed that even within the common region, some minutiae detected in one image may not be detected in another image due to different image qualities. Due to these reasons, when any two of these three images are used for matching in a fingerprint identification or verification system, false rejection would occur when the threshold related to the total number of matched minutiae pairs is set rather high.

Fig. 6 shows the synthesized minutiae points collected from Figures 3-5, using Fig. 3 as the background image.

Table 1: Sum of Squared Errors for fit and test data

Sum of squared error for fit data			
	Affine	Projective	Nonlinear
Mean	31.1304	62.2254	16.4531
STD	25.3905	87.7418	19.4167
Sum of squared error for test data			
	Affine	Projective	Nonlinear
Mean	28.2344	227.7379	464.9472
STD	29.7245	428.2317	1559.9000

The 'circles' in the figure indicates the original detected minutiae points from Fig. 3, whereas the 'plus' and 'stars' indicate those additional minutiae points transferred from Fig. 4 and Fig. 5 respectively. As seen from Fig. 6, these additional minutiae points have found correct correspondences on the fingerprint image (Fig. 3) which are not detected in the original capture. A match comparing a query image data with minutiae data from Fig. 6 will have a higher matching count.
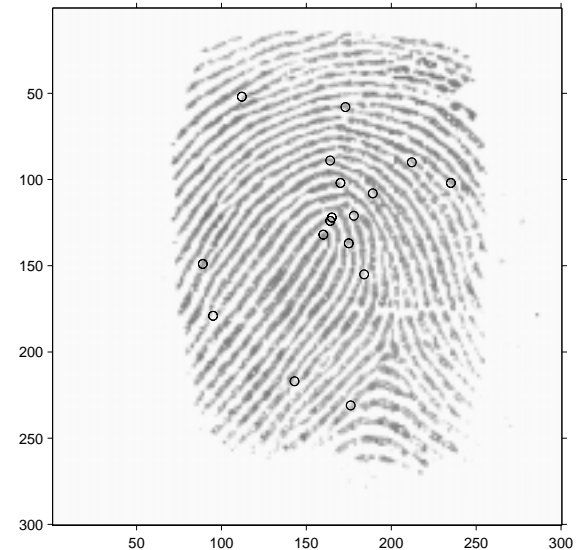
Figure 3: Fingerprint sample 1 with detected minutiae

5.3 Performance evaluation

In this experiment, we show that the fingerprint synthesis method can improve performance in terms of False Rejection caused by using different regions of fingerprints for matching. A test sample consisting of 115 query images and 6×115 template images were used for matching evaluation. The query images were randomly acquired from different partial regions of a finger of each individuals. The first five sets (labeled as (a)-(e)) of template images consist of different partial regions (i.e. centre, top-left, top-right, bottom-left, bottom-right) from each enrolled finger. The last set (label as (f)) of templates consists of synthesized data which are obtained by merging those corresponding data from the same finger of the first five sets. As such, the last set of templates contains the same number of records as those in the first five sets, but with richer information.
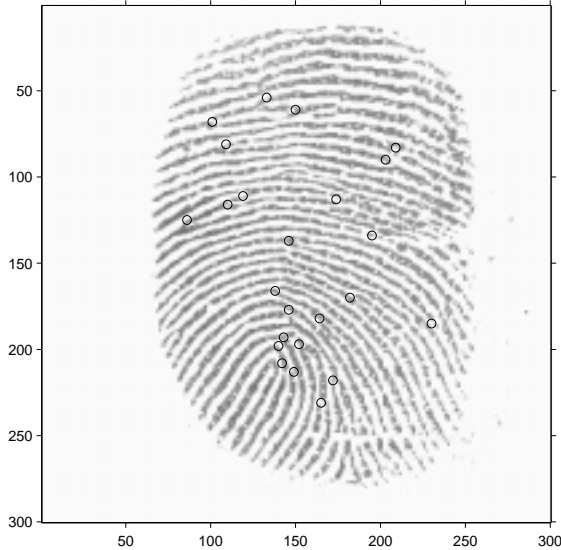
Figure 4: Fingerprint sample 2 with detected minutiae
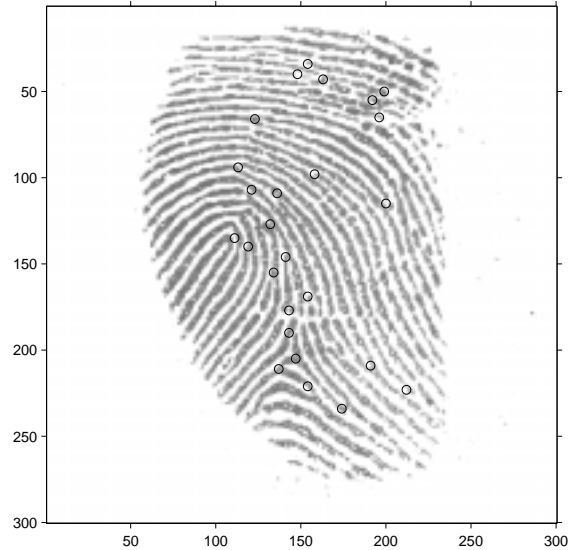
Figure 5: Fingerprint sample 3 with detected minutiae

In Table 2, the percentages of match between the query image data set with each of the six template data sets are shown. It is seen that the synthesized data set (f) has provided the highest percentage of match for similar fingers.

The number of matched minutiae pairs are also plotted in Fig. 7 for all test samples. In this figure, the solid line represents the distribution of the number of matched minutiae pairs corresponding to the synthesized template set (f) while all other dotted lines represent the distribution corresponding to template sets (a)-(e). It is seen from this figure that the number of matched minutiae pairs (solid line) provides almost a covering envelope for the synthesize template set over all other template sets. This indicates that most of the synthesized data set has successfully captured the required minutiae information from individual template data set. Those 'uncovered' cases corresponds to much distorted information due to incorrect as well as inaccurate transformation as a result of the matching process. It is thus noted that obtaining as much matching minutiae pairs before synthesizing the data could possibly help to improve the situation.

Table 2: Percentage of match for each template set

Data sets					
(a)	(b)	(c)	(d)	(e)	(f)
57.39%	50.88%	54.95%	41.12%	36.79%	80.00%

6 Conclusion

In view of the limitation in solid state image sensor area, we propose, in this paper, a method to synthesize fingerprint data. The method is advantages over existing mosaicing technique in terms of low computational cost and low memory storage requirements. Several transformation models were compared for minutiae points alignment. The affine transformation, which was found to provide good interpolation and extrapolation capabilities,

was adopted for minutiae data synthesis. The synthesized template data set was found to improve matching performance in the sense of reducing false rejection which was caused by using different fingerprint regions of the same finger for matching.

References

[1] Anil Jain, Lin Hong, and Ruud Bolle, "On-line fingerprint verification", IEEE Trans. Pattern Analysis and Machine Intelligence, vol. 19, no. 4, pp. 302–313, 1997.

[2] Anil K. Jain, Lin Hong, Sharath Pankanti, and Ruud Bolle, "An identity-authentication system using fingerprints", in Proceedings of the IEEE, 1997, pp. 1365–1388.

[3] Nalini K. Ratha, Kalle Karu, Shaoyun Chen, and Anil K. Jain, "A real-time matching system for large fingerprint databases", IEEE Trans. Pattern Analysis and Machine Intelligence, vol. 18, no. 8, pp. 799–812, 1996.

[4] U. Halici, L. C. Jain, and A. Erol, "Introduction to fingerprint recognition", in Intelligent Biometric Techniques in Fingerprint and Face Recognition, L. C. Jain and et. al., Eds., pp. 3–34. The CRC Press international series on computational intelligence, 1999.

[5] Lawrence O'Gorman, "Fingerprint verification", in Biometrics: Personal Identification in Networked Society, Anil K. Jain, Ruud Bolle, and Sharath Pankanti, Eds., 1999, pp. 43–64.

[6] Nalini K. Ratha, Jonathan H. Connell, and Ruud M. Bolle, "Image mosaicing for rolled fingerprint construction", in 14th International Conference on Pattern Recognition, 1998, vol. 2, pp. 1651–1653.

[7] Raffaele Cappelli, Alessandra Lumini, Dario Maio, and Davide Maltoni, "Fingerprint classification by directional image partitioning", IEEE Trans. Pattern Analysis and Machine Intelligence, vol. 21, no. 5, pp. 402–421, 1999.

[8] Anil K. Jain and Lin Hong, "A multichannel approach to fingerprint classification", IEEE Trans. Pattern Analysis and Machine Intelligence, vol. 21, no. 4, pp. 348–359, 1999.

[9] Kalle Karu and Anil K. Jain, "Fingerprint classification", Pattern Recognition, vol. 29, no. 3, pp. 389–404, 1996.

[10] Ugur Halici and Güclü Ongun, "Fingerprint classification through self-organizing feature maps modified to
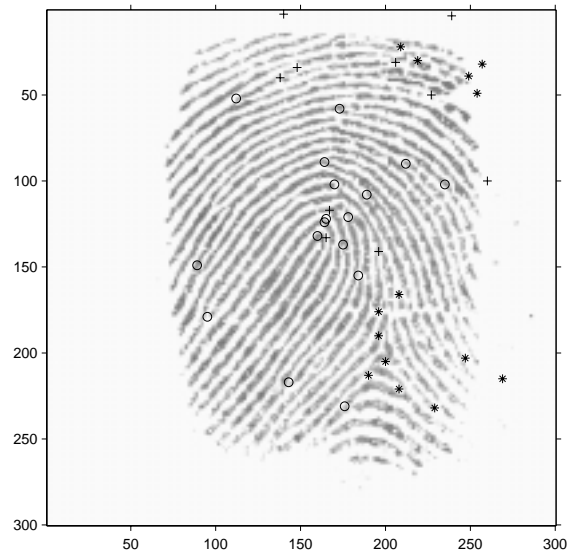
Figure 6: Fingerprint sample with synthesized minutiae (o: from samlpe 1; +: from sample 2; *: from sample 3)
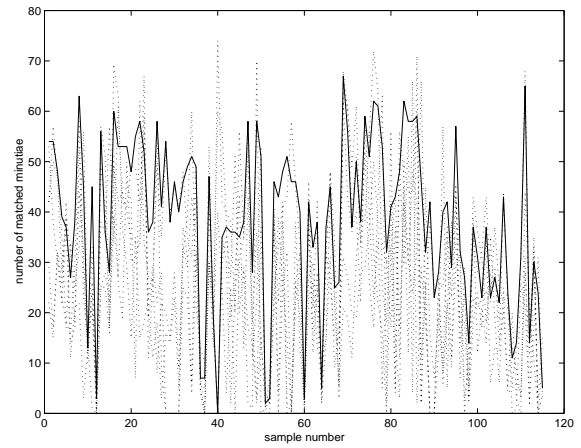
Figure 7: Distribution of number of matched minutiae for each test sample

treat uncertainties", in Proceedings of the IEEE, 1996, pp. 1497–1512.

[11] U.S. Government Printing Office, Washingtion, D. C., The Science of Fingerprints: Classification and Uses, 1984.

[12] H. C. Lee and R. E. Gaensslen, Eds., Advances in Fingerprint Technology, Elsevier, New York, 1991.

[13] Xudong Jiang and Wei Yun Yau, "Fingerprint minutiae matching based on the local and global structures", in 15th Internaional Conference on Pattern Recognition, 1999.

[14] D. Maio and D. Maltoni, "Direct gray-scale minutiae detection in fingerprints", IEEE Trans. Pattern Analysis and Machine Intelligence, vol. 19, no. 1, pp. 27–40, 1997.

[15] Xudong Jiang, Wei Yun Yau, and Wee Ser, "Minutiae extraction by adaptive tracing the gray level ridge of the fingerprint image", in IEEE Internaional Conference on Image Processing (ICIP'99), 1999, pp. 852–856.